Coordinated perimeter flow and variable speed limit control for mixed freeway and urban networks

By

Rebeka Yocum
Department of Civil and Environmental Engineering
The Pennsylvania State University
201 Transportation Research Building
University Park, PA 16802
Phone: 814-863-1897
rly16@psu.edu

Vikash V. Gayah*
Department of Civil and Environmental Engineering
The Pennsylvania State University
231L Sackett Building
University Park, PA 16802
Phone: 814-865-4014
gayah@engr.psu.edu

***Corresponding Author**

July 2020

Word Count: 6,124 (5,874 words + 1 table)

ABSTRACT

Recent studies have leveraged the existence of network Macroscopic Fundamental Diagrams to develop regional control strategies for urban traffic networks. Existing strategies—such as perimeter metering control, which limits how vehicles are able to move between regions of an urban network—primarily focus on controlling traffic on urban streets and do not consider how freeway traffic can be controlled to improve overall traffic operations in mixed freeway and urban networks. The purpose of this study is to develop another coordinated traffic management scheme that simultaneously implements perimeter flow control on the urban network and variable speed limits on the freeway to reduce total travel time in such a mixed network. Variable speed limits slow down vehicles traveling along the freeway, which effectively serves as a surrogate form of metering traffic exiting the freeway into the urban network. Slowing down vehicles on the freeway can be useful since freeways often have large storage capacities and vehicles accumulating on freeways might be less disruptive to overall system operations than on urban streets. The combined control strategy is implemented in a model predictive control framework with several realistic constraints, such as gradual reductions in freeway speed limit. Numerical tests suggest that the combined implementation of variable speed limits and perimeter metering control can improve traffic operations compared to perimeter metering alone, and that variable speed limits alone might be beneficial in some scenarios where perimeter metering control is not able to effectively reduce total network travel time.

INTRODUCTION

Management of freeway and surface streets is a topic of great interest to the traffic flow community. A variety of strategies have been proposed and tested to improve traffic performance on freeways, including on-ramp metering (*1–3*) and variable speed limits (*4–6*), among others. These congestion management strategies are often applied to mitigate congestion on individual freeway bottlenecks. On the urban street side, control strategies generally focus on adjusting signal timings at individual intersections (*7–10*) , since signals serve as the most common bottlenecks on urban streets. Isolated urban networks and freeways are not representative of the mixed networks that exist in which freeways and urban networks interact. It is beneficial to consider congestion management strategies that control vehicles across these different roadway types. However, coordinating traffic management across freeways and urban streets has generally been difficult due to the complexity of describing traffic across these different roadway types using traditional methods.

Recent advances in modeling large-scale urban traffic networks may serve as a bridge to coordinate traffic control across freeways and urban networks as they provide a more computationally efficient way to describe traffic behavior from a regional perspective. These methods rely on the existence of well-defined relationships between traffic variables across spatially compact regions (*11–13*)—known more commonly as network Macroscopic Fundamental Diagrams (NFDs or MFDs)—that arise under certain conditions (*14*, *15*). Leveraging knowledge of these MFDs to model urban traffic network dynamics (*16*) allows for the development of elegant network-wide congestion management strategies in which entire networks can be managed without controlling individual intersections within the region. Previous studies have implemented MFD-based frameworks to develop various regional-level urban traffic control strategies. Examples of these strategies include perimeter flow control/metering (*17–22*), pricing (*23–26*), and street network design (*27–30*), among others (*31*, *32*).

To the authors' knowledge, only one study used an MFD-based framework to develop a coordinated traffic management scheme for freeways and urban networks (*33*). Perimeter flow control and on-ramp metering were simultaneously implemented to improve reduce the combined total travel time experienced on both. The proposed strategy determined optimal rates vehicles were allowed to travel between regions of an urban network (perimeter flow control/metering), as well as rates vehicles were allowed to move between the urban network and freeway (on-ramp metering). The combination of this joint freeway/urban network control was found to improve traffic conditions on the combined network. However, this strategy only limited vehicle movement between the urban regions and from the urban region to the freeway, and it did not consider limiting vehicle movement from the freeway to the urban network. Thus, an important piece is missing from the previous work surrounding congestion management in mixed networks: managing the vehicles exiting the freeway and entering the urban region.

The purpose of this study is to develop a coordinated traffic management scheme that simultaneously implements perimeter flow control on the urban network and variable speed limits on the freeway. As will be shown, variable speed limits can be used as a means to limit how vehicles are able to move from the freeway to the urban network, which can serve as a surrogate form of metering. While a similar effect can be achieved by metering the rate vehicles can exit the freeway (either at the ramp location or downstream where the ramp connects with the surface streets), VSL control does not require vehicles from the freeway to completely stop, which could

lead to long queues and unnecessary congestion or queue spillover to freeway itself. Instead, it simply changes the speed and density at which vehicles travel along the freeway. This might be useful in specific situations since freeways often have large storage capacities and vehicles accumulating on freeways might be less disruptive than vehicles accumulating on urban streets. In this paper, we integrate the combined VSL-perimeter metering control into an MPC optimization framework for networks governed by MFDs. The framework is used to compare the effectiveness of VSL control, perimeter metering control, and a combination of the two as a means to manage congestion in a mixed network made up of urban regions and a freeway.

The remainder of this paper is organized as follows: first, the methodology is outlined; then, three numerical examples are presented; finally, a discussion of the results and future work is provided.

METHODOLOGY

In this work, we consider a system that consists of a freeway and an urban network, the latter of which can be partitioned into two homogenous urban regions (e.g., an inside and outside region). Such partitioning has been shown to produce more reliable and well-defined MFDs (*34*). A schematic representation of this system is shown in Figure 1. For computational simplicity, a single off-ramp exists through which vehicles can exit the freeway and travel to the inside region. Freeway vehicles destined for the outside region but first exit to the inside region and then travel from the inside to outside region. Note, however, that the proposed method is general and can accommodate off-ramps providing access to both regions. However, this is excluded from this study since it would introduce additional complications, namely vehicle route choice. Methods to address route choice for freeway vehicles have already been developed and these existing methods can be readily integrated into the proposed framework; see (*33*) for more details.

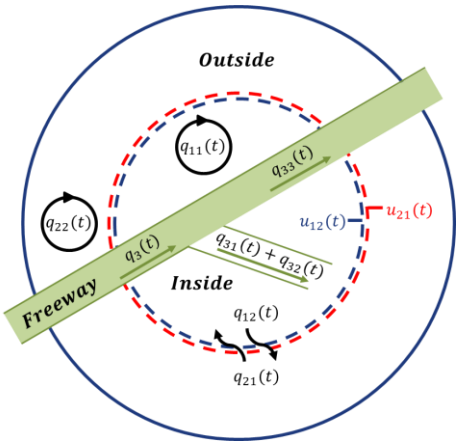

Figure 1. Schematic representation of the two urban region and freeway network

Traffic within the two urban regions ($i = 1$ for inside region, $i = 2$ for outside region) is assumed to be described by well-defined MFDs that relate accumulation in region i, $n_i(t)$, with

the trip completion rate in that region, $G_i(n_i(t))$. Vehicle movement between the two urban regions is managed using perimeter metering control. The controllers, expressed as $u_{12}(t)$ and $u_{21}(t)$, limit the proportion of vehicles wishing to move between the two regions that are actually able to do so. For example, a control value of $u_{12}(t) = 0.6$ means that 60% of vehicles that wish to move from the inside region to the outside region are permitted to do so while the other 40% are held back and can only transfer between the two regions at a later time. Traffic on the freeway ($i = 3$) is managed using variable speed limits (VSL) where a speed limit is implemented at each time step, t. The effect of the implementation of VSL on freeway traffic will be described in the next section.

The inside and outside regions experience endogenous demands expressed as $q_{11}(t)$ and $q_{22}(t)$, respectively, and exogenous demands expressed as $q_{12}(t)$ and $q_{21}(t)$, respectively. We assume that the freeway operates in free flow and no active bottlenecks exist. The total freeway demand is expressed as $q_3(t)$, with some portion of vehicles exiting the freeway into the urban network and the remaining vehicles continuing on. Freeway vehicles that enter the urban network are either destined for the inside or outside region, and the corresponding demands are expressed as $q_{31}(t)$ and $q_{32}(t)$, respectively. The demand that does not exit the freeway is expressed as $q_{33}(t)$ where:

$$q_3(t) = q_{31}(t) + q_{32}(t) + q_{33}(t). \quad (1)$$

Implementation of variable speed limits

The effect of variable speed limit control on free flow freeway traffic is predicted using LWR theory (*35–38*). We assume traffic on the freeway can be described using a triangular fundamental diagram (FD), as illustrated in Figure 2a. We also assume the VSL control is implemented within a specific "zone" along the freeway and that speeds are only allowed to change at discrete points in time. These spatial and temporal constraints allow us to estimate the impact of changing the speed limit on freeway traffic graphically using time space diagrams. It is assumed that all vehicles obey the VSL guidance and are aware of speed limit changes as they are made. Such VSL implementation could be achieved using regularly spaced dynamic VSL signs or using Connected Vehicle technology (*6*). The effects of non-compliance could be integrated by modeling only the change in average speed and selecting the corresponding speed limit that would achieve the desired average travel speed. Note that previous research has found small changes in speed limit would generally be accepted by travelers, while larger reductions in speed limit are more likely to be ignored (*39*).

Under these assumptions, changes in speed limit at a point in space are represented by a horizontal interface on the time space diagram, and changes in speed limit at a point in time are represented using a vertical interface on the time space diagram, similar to the work presented in (*35*). Consider a known freeway traffic demand, where vehicles are traveling in free-flow conditions. A lower speed within a specific region of time and space results in traffic states that are associated with a second free flow branch on the FD, as shown in Figure 2b. Thus, lowering the speed limit should generate three interfaces: one horizontal, one vertical, and one traveling at the newly implemented speed limit. An example of these interfaces are illustrated as dark red lines on the time space diagram that accompanies the FD in Figure 2b. The lighter lines represent individual vehicle trajectories and how they would change in response to the changes in the speed

limit. Notice that lowering the speed limit causes an initial reduction in flow as vehicles within the lower-speed limit zone reduce their speed but maintain their density. However, the flow of vehicles entering at the reduced-speed limit stays the same as vehicles simply adjust their speed and corresponding travel density upon entering this section,.

Similar interfaces arise when the speed limit is increased; see Figure 2c. Traffic states only arise on a new free-flow branch of the FD associated with the increased speed. Note that this is equal to the original free-flow branch if the increased speed is equal to the original free-flow speed, but could also result in a new free flow branch if the increased speed limit is smaller than the free-flow speed. Three interfaces again arise when the speed limit is increased: one horizontal, one vertical, and one traveling at the newly implemented speed limit. An example of this transition is shown in Figure 2c. The figure reveals that when the speed limit is increased, the first few vehicles travel at the same density and a higher speed, resulting in a momentary increase in flow, while the following vehicles maintain their flow while traveling at a lower density.

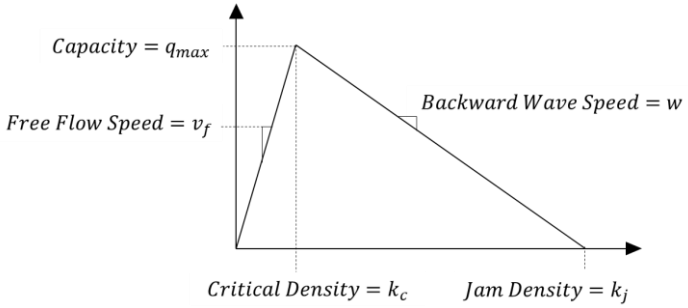

(a) Assumed triangular fundamental diagram

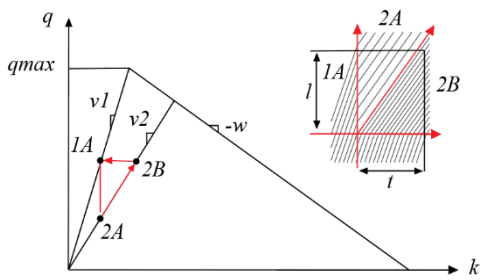

(b) Reduction in speed limit

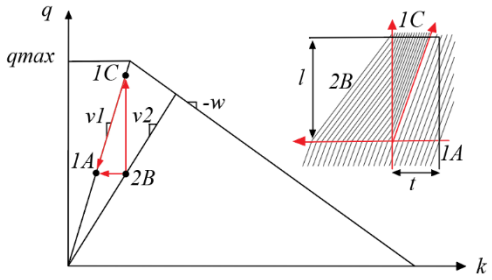

(c) Increase in speed limit

Figure 2. Assumed triangular fundamental diagram and traffic states that arise when speed limit is reduced and increased

A minimum speed limit can be determined to ensure that the freeway flow does not become congested when a lower speed limit is increased. This lower bound ensures that the point 1C in Figure 2c will never lie on the congested branch of the fundamental diagram and is a function of freeway demand, free flow speed, v_f, and the capacity of the freeway, q_{max}:

$$v_{min} = \frac{q_3(t) * v_f}{q_{max}} \quad (2)$$

Assuming that the exit ramp into the urban network lies at the end of the VSL zone allows us to calculate the average flow passing the exit ramp during any discrete time period as the

proportion of time each state occurs on the time space diagram.The length of the VSL zone is determined to ensure that the impact of changing the speed limit during a given time period on traffic flow is fully contained within that time period. This length is:

$$l \leq \frac{q_3(t)*v_f}{q_{max}} t, or\ l \leq v_{min} t \quad (3)$$

Under these conditions, the flow on the freeway during time period t can be described as a function of the freeway demand, the speed limit in the previous time period and the speed limit implemented in time period t:

$$q_{ramp}(t) = f(q_3(t), v_{des}(t-1), v_{des}(t)) \quad (4)$$

The flow passing the exit ramp is calculated using the proportion of time that each traffic state exists at the exit ramp. Considering the speed limit reduction shown in Figure 2b, the flow passing the exit ramp is calculated as shown below.

$$q_{ramp} = \left(q_{2A} * \frac{\frac{l}{v_2}}{t}\right) + \left(q_{2B} * \frac{t - \left(\frac{l}{v_2}\right)}{t}\right),$$

where $q_{2A} = k_{2A} * v_2 = \frac{q_{1A}}{v_1} * v_2$ and $q_{2B} = q_{1A}$. Simplification results in the final expression for the ramp passing the exit ramp;

$$q_{ramp} = q_{1A}\left(1 + \left(\frac{l}{t*v_1}\right) - \left(\frac{l}{t*v_2}\right)\right).$$

Without loss of generality, consider a case where there are three possible speed limit alternatives (v_1, v_2, v_3) and a constant freeway demand, where $q_3(t) = q_3(t+1) = q_3\ \forall\ t$. With these assumptions, the flow passing the exit ramp during any time step $t+1$ can be represented in a matrix form as a function of the demand (q_3), speed limits in the current $(v(t))$ and future $(v(t+1))$ time steps and the length of the time interval (Δt); see Table 1. These values are obtained from the geometry of Figure 2b and Figure 2c.

Table 1. Matrix representation of the possible values of freeway flow passing the exit ramp

Speed Limit at Current Time Step (t) \ *Speed Limit at Next Time Step (t + 1)*	$\mathbf{v_1}$	$\mathbf{v_2}$	$\mathbf{v_3}$
$\mathbf{v_1}$	q_3	$q_3\left[1+\left(\frac{l}{\Delta t * v_1}\right)-\left(\frac{l}{\Delta t * v_2}\right)\right]$	$q_3\left[1+\left(\frac{l}{\Delta t * v_1}\right)-\left(\frac{l}{\Delta t * v_3}\right)\right]$
$\mathbf{v_2}$	$q_3\left[1+\left(\frac{l}{\Delta t * v_2}\right)-\left(\frac{l}{\Delta t * v_1}\right)\right]$	q_3	$q_3\left[1+\left(\frac{l}{\Delta t * v_2}\right)-\left(\frac{l}{\Delta t * v_3}\right)\right]$
$\mathbf{v_3}$	$q_3\left[1+\left(\frac{l}{\Delta t * v_3}\right)-\left(\frac{l}{\Delta t * v_1}\right)\right]$	$q_3\left[1+\left(\frac{l}{\Delta t * v_3}\right)-\left(\frac{l}{\Delta t * v_2}\right)\right]$	q_3

This representation allows for a simple mathematical relationship that can be used to estimate the effect of changing the speed limit on the freeway on traffic flow. The matrix in Table 1 can also be expanded to account for a changing freeway demand, as well as more than three possible speed limits. However, differences along the diagonal would have been be incorporated to address the situations where changes passing the exit ramp might occur without an accompanying change in speed limit. The equations in Table 1 can be generalized to account for a changing freeway demand, shown in equation (5).

$$q_{ramp}(t) = q_3(t) + \frac{q_3(t-1)*l}{\Delta t * v(t-1)} - \frac{q_3(t)*l}{\Delta t * v(t)} \quad (5)$$

The flow $q_{ramp}(t)$ is then split by destination according to the destination of the original freeway demands (inside region, outside region, continuing on freeway) as shown in Equations (7, 8, 13-15) below.

Optimal control problem

The combined VSL and gating control problem becomes a mixed integer nonlinear program (MINLP). The proposed control problem can be solved using an MPC framework as described in (*40*). The MPC framework is a receding horizon framework in which the controller looks far into the future at every time step and determines an optimal set of steps to take; however, only the first set of control actions in the optimal sequence is implemented. Then, the optimization process repeats itself to determine the next set of control actions to implement. The number of time steps that the controller considers in determining the impact of the control during the optimization is the prediction horizon, N_p. Optimal control actions are only obtained for the first subset of these time steps, which is known as the control horizon, N_c. Following (*40*), we use a prediction horizon of twenty time steps and control horizon of two time steps in the MINLP presented in this paper.

Every time the MPC controller solves for an optimal sequence of control actions, it considers the effect of these actions on a given objective function. The objective function considered in this work is the minimization of the total number of vehicles within the network (and thus, minimizes the total travel time) observed during some study period t_0 through t_f. This objective function is mathematically represented by:

$$J = \min_{u_{21} u_{12}, v_{des}} \int_{t_0}^{t_f} [\sum n_i(t)] dt, \quad (6)$$

where $\sum n_i(t), i = 1,2,3$ represents the total accumulation in the mixed network during time period t, $n_i(t) = \sum n_{ij}(t), i,j = 1,2$, is the accumulation in region i, $n_3(t) = \sum n_{3k}, k = 1,2,3$ is the accumulation on the freeway, and $v_{des} \in \{v_1, v_2, \dots, v_n\}$ is the variable speed limit chosen from a discrete set of values. Discrete values for the speed limit are chosen to ensure implemented speed limits are not unusual and do not cause confusion to those traveling on the freeway.

Dynamic equations similar to those in (*33*) are used to describe how accumulations within each region change over time. First, it is beneficial to define the parameters below.

$\beta \in (0,1)$	portion of total freeway demand wishing to continue on the freeway
$\alpha_1 \in (0,1)$	portion of total freeway demand wishing to end up in the inside region
$\alpha_2 \in (0,1)$	portion of total freeway demand wishing to end up in the outside region

Note that $\beta + \alpha_1 + \alpha_2 = 1$, and all vehicles exiting the freeway must enter the inside region regardless of where they intend to complete their trip because there is no direct exit ramp from the freeway into the outside region.

Equations (7-8) provide the dynamic equations that show how accumulation of vehicles within the inside region destined for the inside region, and the outside region changes in time. Equations (9-10) provide the dynamic equations that show how accumulation of vehicles within the outside region destined for the outside region and the inside region changes in time. Equations (11-13) show how the accumulation of vehicles on the freeway destined for the inside, and outside regions changes, as well as how the accumulation of vehicles not wishing to exit the freeway changes.

$$\frac{dn_{11}(t)}{dt} = [q_{11}(t) - M11(t) + u_{21} M21(t) + \alpha_1 * q_{ramp}(\mathrm{t})] \quad (7)$$

$$\frac{dn_{12}(t)}{dt} = [q_{12}(t) - u_{12} M12(t) + \alpha_2 * q_{ramp}(t)] \quad (8)$$

$$\frac{dn_{22}(t)}{dt} = [q_{22}(t) - M22(t) + u_{12} M12(t)] \quad (9)$$

$$\frac{dn_{21}(t)}{dt} = [q_{21}(t) - u_{21} M21(t)] \quad (10)$$

$$\frac{dn_{31}(t)}{dt} = [q_{31}(t) - \alpha_1 * q_{ramp}(t)] \quad (11)$$

$$\frac{dn_{32}(t)}{dt} = [q_{32}(t) - \alpha_2 * q_{ramp}(t)] \quad (12)$$

$$\frac{dn_{33}(t)}{dt} = [q_{33}(t) - \beta * q_{ramp}(t)] \quad (13)$$

The MFD is used to describe how vehicles move between regions in the urban network or complete their trip. $M_{11}(t)$ and $M_{22}(t)$ represent the rate at which travelers complete their trips within the inside and outside regions, respectfully, and are shown in Equations (14-15). The summation of $M_{11}(t) + M_{22}(t)$ yields the rate at which vehicles complete their trips within the entire urban network. $M_{12}(t)$ and $M_{21}(t)$ are the transfer functions from the inside to outside region and outside to inside region in time period t, which represent the rates at which vehicles switch between regions, and are expressed in Equations (16-17).

$$M_{11}(t) = \left(\frac{n_{11}(t) * G_1(n_1(t))}{n_1(t)}\right) \quad (14)$$

$$\mathrm{M}_{22}(\mathrm{t}) = \left(\frac{n_{22}(t) * G_2(n_2(t))}{n_2(t)}\right) \quad (15)$$

$$M_{12}(t) = \frac{n_{12}(t) * G_1(n_1(t))}{n_1(t)} \quad (16)$$

$$M_{21}(t) = \frac{n_{21}(t) * G_2(n_2(t))}{n_2(t)} \quad (17)$$

NUMERICAL RESULTS

Three case study examples are now used to illustrate the benefits of VSL and combining VSL with gating, as well as testing the stability of the proposed control to fluctuations in travel demand and the MFD. For the purposes of this study, both regions are assumed to share the same MFD, which is a re-scaled and adjusted version of the MFD for Yokohama, Japan as provided in (*40*). The congested branch is specifically adjusted so it is linear so that the MFD is concave and is equal to zero at the jam accumulation. Heavily congested regions are not considered in this paper and as such, this assumption does not impact any of the examples.

The functional form of the MFD considered is:

$$G(n(t)) = \begin{cases} \left((2.052e^{-7} * n^3) - (2.586e^{-3} * n^2) + (9.58 * n)\right), & 0 < n < 4{,}666 \\ \left(15{,}714.233 - (1.38655 * n)\right), & 4{,}667 < n < 11{,}333 \end{cases} \quad (18)$$

From Equation (18) we see that the critical accumulation in each region is $2{,}710\ veh$ and this is associated with a maximum trip completion rate of $3.07\ veh/sec$. The maximum accumulation in each region is $11{,}333\ veh$.

Traffic on the freeway is assumed to obey a fundamental diagram with free flow speed of 60 mi/hr, capacity of 8,800 veh/hr and backward wave speed of -10 mi/hr. A constant time-step of $\Delta t = 1$ minute is assumed with a control horizon of $N_c = 2$ time steps and a prediction horizon of $N_p = 20$ time steps when implementing the MPC framework. Furthermore, adopted speed limits are assumed to be held constant for at least 5 minutes to ensure that speed limits do not change too

rapidly. Finally, speed limits are assumed to change gradually (e.g., in 10 mi/hr increments) to avoid sudden speed changes, and are restricted to three possible values (specifically 60, 50, and 40 mi/hr). Additional constraints are added to ensure lower and upper bounds of the accumulations within each region, and minimum and maximum control constraints are met. These constraints are shown below.

0	minimum accumulation in the urban regions
11,333	maximum accumulation in the urban region
0.1	minimum perimeter control constraint
0.9	maximum perimeter control constraint

The optimization problems are solved heuristically using particle swarm optimization. Since its introduction in 1995 (*41*), the PSO algorithm has been adjusted to suit a variety of needs. It has proven to be effective at solving single objective and multi objective, mixed integer nonlinear programs (*42*) and is popular due to its low computational cost and the speed at which it can be implemented. Extensive tests were performed to ensure that the PSO was properly tuned so that optimal solutions were achieved for this problem.

Scenario 1: Benefit of VSL Control

The first scenario considers a case in which VSL provides benefits while perimeter metering control will not. This will occur when the congestion in the urban network is primarily due to the demand exiting the freeway, along with a peak in internal and external demands within each urban region. Even though there is a significant demand for trips that are generated in one region and move to another, few vehicles wish to cross the border between the two regions at the beginning of the study period and thus the network becomes congested even if transfer flows between the two regions could be completely shut down. We expect VSL control alone to be more effective at managing the congestion than perimeter metering control in such a case because there are few vehicles traveling between regions, and thus limiting flow between regions will not have a large impact on overall network operations. Figure 3a provides the demand profile adopted for the first numerical test. All exogeneous and endogenous urban network demands are assumed to peak over the course of a 20-minute period, mimicking a morning rush.

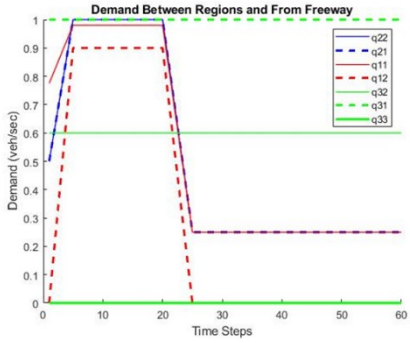

(a) Demands used in the first numerical simulation

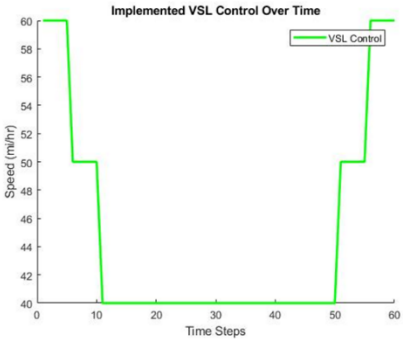

(b) Speed Limit VSL Control Only

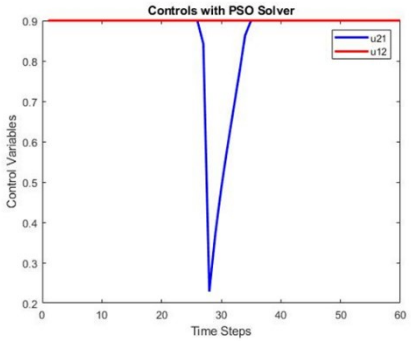

(c) Perimeter Metering Control Implemented Only

Figure 3. Demands, and different types of control used in the first numerical simulation

Figure 4 shows accumulations within the two urban network regions and on the freeway under three scenarios: no control, VSL only and gating only, along with the total travel time in each scenario. The results reveal that in this scenario, perimeter metering control is not effective at managing congestion within the network, while the implementation of VSL control alone is effective at lowering total travel time.

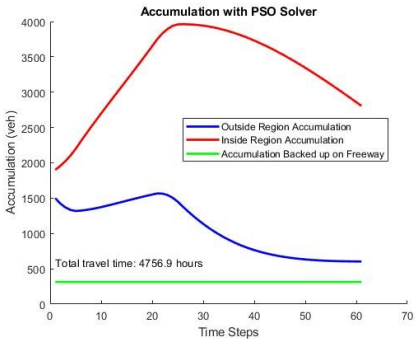

(a) No control (TTT = 4,756.9 veh-hr)

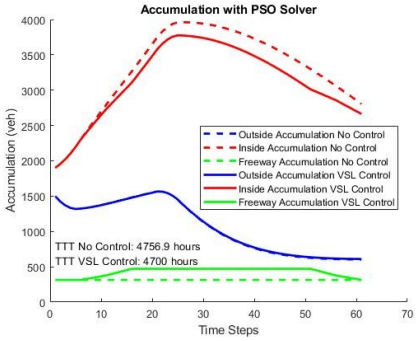

(b) VSL alone (TTT = 4,700 veh-hr)

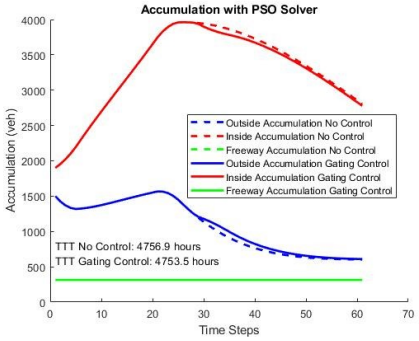

(c) Gating alone (TTT = 4,753.5 veh-hr)

Figure 4. Accumulations and total travel time under different scenarios.

The time series of accumulation over time for the case when no control is implemented is shown in Figure 4a. Due to the constant demand exiting the freeway as well as the spike in internal demands in the inside region, the inside region slowly becomes congested. Congestion occurs once the accumulation in the region surpasses the critical accumulation observed in the MFD, around 2,710 vehicles. The outside region experiences a peak in accumulation but remains uncongested for the duration of the study period. During the hour-long study period, travelers experience a total of 4,756.9 vehicle-hours of total travel time.

Now, consider the scenario in which VSL is implemented on the freeway in an attempt to manage the congestion in the mixed network. A plot of how the speed limit changes over time is shown in Figure 3b. Note that the speed limit is reduced in two 10 mph increments, which is done to ensure drivers do not experience a large change in speed limit at any one point in time. Considering Figure 3b and Figure 4b, we can see that once the accumulation in the inside region surpasses a critical accumulation (at time step 15), the demand on the freeway is momentarily limited by two successive decreases in speed limit. This provides the inside region time to relieve some of the congestion caused by the large spike in internal demands happening around that same time, as shown in Figure 3a. Shortly after the inside region becomes uncongested once again (around time step 50), the speed limit on the freeway is stepped back up to the original value of sixty miles per hour. While this causes the flow into the internal region to increase and results in a corresponding increase in accumulation in the inside region at this time, this actually serves to benefit network operations. Specifically, the increase in flow occurs when it will be associated

with an increase in the trip completion rate within the inside region. With VSL control implemented, travelers experience 4,700 vehicle-hours of total travel time, approximately a 1.2% reduction from the no control scenario.

Now, consider the same case study when only perimeter metering control is implemented. Previous work has shown that perimeter metering control is effective in managing congestion within and between two urban regions (*40*). However, this congestion management method is not effective when the demand between urban regions is low and both regions are congested. As seen in Figure 3c, perimeter metering is barely implemented during the study period so the total travel time in this scenario is reduced to just 4,753.5 vehicle-hours (less than 0.1% reduction). This example supports the notion that VSL is a viable option to limit congestion within the network in certain scenarios where perimeter metering may not be effective.

Scenario 2: Benefit of Coordinated Control

While the implementation of VSL control and perimeter metering control has been shown to be beneficial on their own, in certain circumstances, a combination of the two can have cumulative benefits. The second scenario is a case where the coordination of perimeter metering and VSL control is more effective at managing congestion within the network than either strategy on its own. Consider an adjustment to the previous numerical example: there is now a large spike in demand from the outside region into the inside region, and a smaller spike in internal demands. In this case, perimeter metering control on its own is more effective at lowering total travel time than VSL control is on its own, but the combination of the two proves to be more effective than either control strategy alone. The demands for this example are shown in Figure 5a. Traffic in the urban regions is described by the same MFD, expressed previously in equation (*18*).

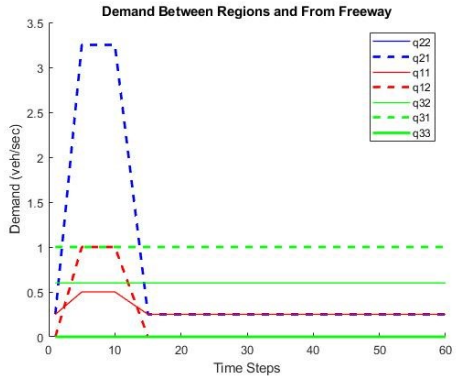

(a) Demands used for the second numerical simulation

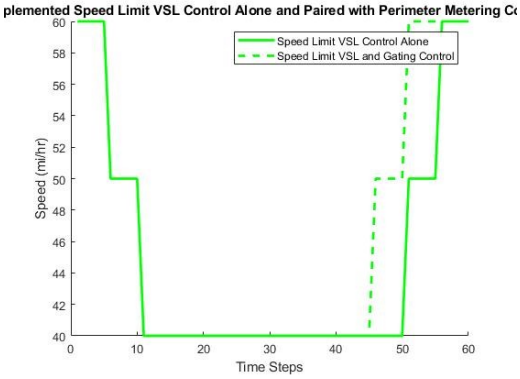

(b) VSL control implemented alone and with perimeter metering control

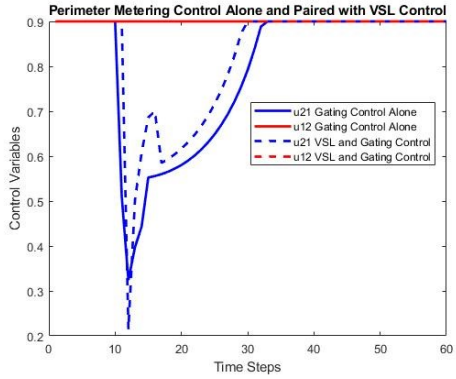

(c) Perimeter metering control implemented alone and with VSL control

Figure 5. Overview of demands, VSL and perimeter metering control used in second numerical simulation

First, we consider the scenario when no control is implemented. In Figure 6a, we can see the accumulation in the inside region increases past the critical accumulation and becomes congested due to the incoming traffic from the freeway, the internal demands, and the demands from the outside to the inside region. The outside region remains uncongested during the study period. Once the demand within and between the urban regions decreases, the inside region slowly becomes uncongested. Without any control implemented, travelers experience 4,498 vehicle-hours of total travel time.

Next, consider the case where VSL control is implemented. Once again, we can see why the control is triggered when comparing the time series of the freeway speed limit (shown in Figure 5b) to the accumulation and the MFD. Compared to the no control scenario, implementing VSL control reduces total travel by approximately 1.3%, as shown in Figure 6b. Similar to the VSL control scenario, the scenario with perimeter metering control only provides a reduction in total travel time compared to the no control scenario of approximately 1.7%, as shown in Figure 6c.

Finally, consider the simultaneous implementation of both VSL and perimeter metering control. Because this case study includes constant demands from the freeway into the inside region, as well as demands from the outside to the inside region, it is expected that a combination of the two control strategies will be more effective than either strategy on its own. Looking at Figure 6d, this is shown to be the case. Combining the two types of control (shown in Figure 5b and Figure

5c) results in a total travel time of 4,400.3 vehicle-hours, which represents a savings in total travel time of about 2.2% compared to the no control scenario. This is a large reduction compared to the no control case (nearly 100 vehicle-hours), and significant reductions compared to VSL alone and perimeter metering alone (over 40 vehicle-hours and over 20 vehicle-hours, respectively).

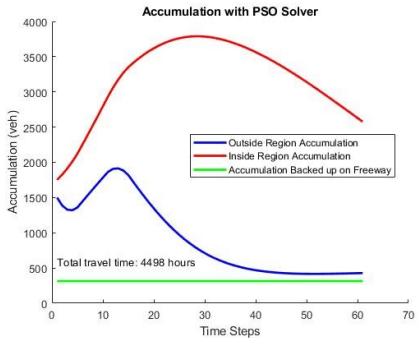

(a) No Control (TTT = 4,498 veh-hrs)

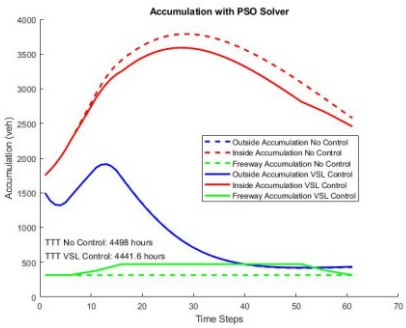

(b) VSL Control Only (TTT = 4,441.6 veh-hrs)

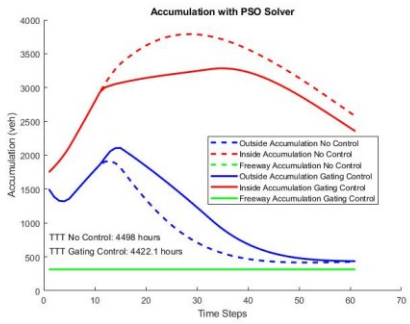

(c) Perimeter Metering Control Only (TTT = 4,422.1 veh-hrs)

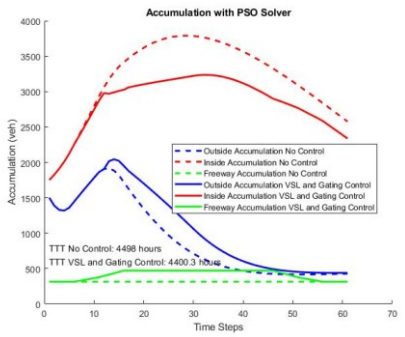

(d) VSL and Perimeter Metering (TTT = 4,400.3 veh-hrs)

Figure 6. Accumulation and total travel time for four different control scenarios

Scenario 3: Stability Test of Second Numerical Example

The previous two examples prove to show that implementation of variable speed limit on its own is effective in managing congestion caused by exiting freeway traffic and that the coordination of VSL and perimeter metering control is even more effective to the same end than implementation of either control on their own. An extension of the second numerical example is shown below to examine the stability of these control strategies when errors are present in the demands and in the MFD that are applied within the optimization framework. To incorporate error into the demands, we assume that the actual demand is equal to the estimated demand that is input into the algorithm plus a normally distributed error term with mean zero and standard deviation equal to three percent of the estimated demand at each time step. The same type of error is added to the MFD, where the standard deviation of the error term is equal to three percent of the average trip completion rate at each time step. This is more realistic than the previous two examples because while we can estimate the average traffic demands and trip completion rates, in real life these values fluctuate randomly. In this more realistic example, the MPC considers average demands and trip completion

rates as presented in the previous two examples, while the real-life simulation operates with errors present in the demand and the MFD. In order to gain a solid understanding of how these control scenarios run considering stochastic demands and MFDs, this example was repeated twenty separate times to determine if the proposed control can still provide travel time savings in a stochastic environment. A sample run of this example for the demands in Scenario 2 is summarized in Figure 7 and Figure 8.

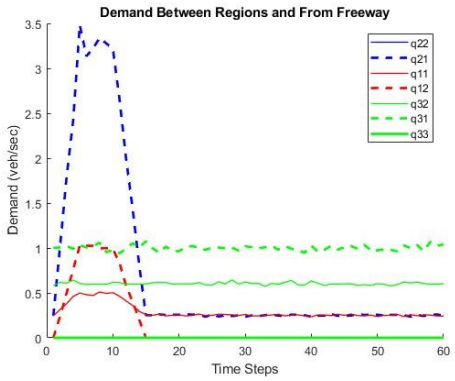

(a) Demands used in the third numerical example

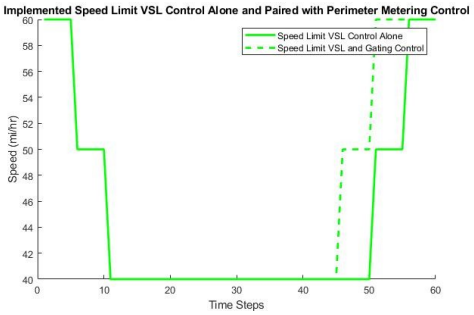

(b) VSL control implemented alone and with perimeter metering control

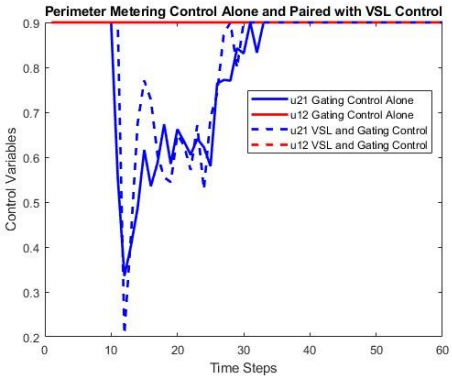

(c) Perimeter metering control implemented alone and with VSL control

Figure 7. Demand used in the third numerical example, and control implemented in different scenarios

Again, we compare the total travel times of four different control scenarios: no control, VSL only, perimeter metering only, and both VSL and perimeter metering control. A sample of the accumulation and total travel time for the four scenarios is shown in Figure 8.

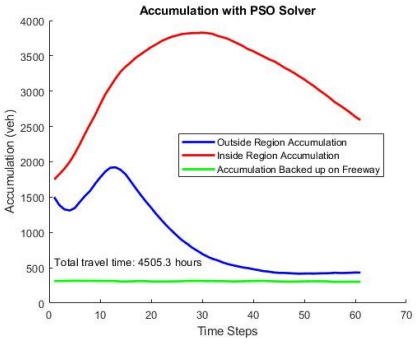

(a) No control (TTT = 4,505.3 veh-hrs)

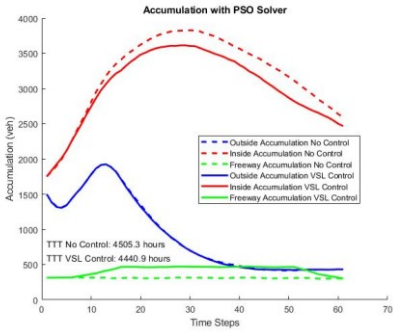

(b) VSL only (TTT = 4,440.9 veh-hrs)

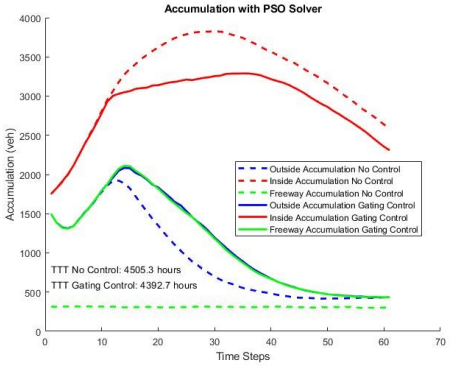

c) Perimeter metering only

(TTT = 4,392.7 veh-hrs)

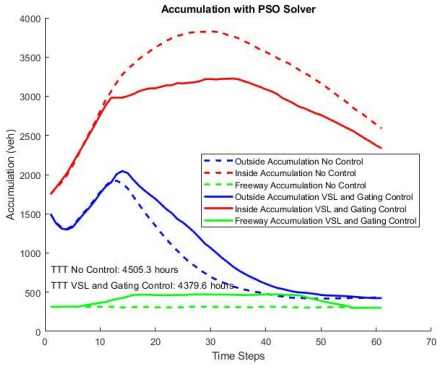

(d) VSL and Perimeter metering control

(TTT = 4,379.6 veh-hrs)

Figure 8. Accumulation and total travel time under different control scenarios

The average total travel times and standard errors for each control scheme are presented below.

No Control:	Mean TTT = 4485.955 veh-hr	Standard Error = 7.407
VSL Control:	Mean TTT = 4440.415 veh-hr	Standard Error = 5.637
Perimeter Metering Control:	Mean TTT = 4416.145 veh-hr	Standard Error = 5.617
Combined Control:	Mean TTT = 4395.515 veh-hr	Standard Error = 6.084

Adding realistic error terms in the demand and the MFD results in different total travel times for all four control scenarios compared to the previous example. The same trends observed in the second numerical example are seen here; implementing VSL control lowers the total travel time compared to the no control scenario, perimeter metering control on its own is more beneficial than VSL control alone, and the combination of VSL and perimeter metering control is more effective at managing congestion than either control strategy alone. All differences are statistically significant and thus not simple due to random fluctuations in demand.

DISCUSSION AND FUTURE WORK

This paper presents a framework for congestion management in a mixed freeway-urban network that applies both perimeter metering control and variable speed limits (VSL). The variable speed limits are used to limit vehicle flow from the freeway to the urban network, which allows vehicles to queue on a freeway instead of on the surface streets where their presence might reduce overall network productivity. The impact of variable speed limits on freeway traffic dynamics are described using kinematic wave theory, which provides the minimum speed limits and length of the freeway over which the variable speed limits must be applied. Reductions in speed limit are found to temporarily reduce the rate vehicles are able to exit the freeway and enter the urban network, while increases in speed limit do the opposite. These changes in flow can be described mathematically, which allows the impacts of VSL to be integrated into an optimization problem to reduce total travel time within the combined network. The joint perimeter control and variable speed limit optimization problem can then be solved using a model predictive control framework. Several numerical tests are performed that demonstrate the scenarios under which 1) VSL would be superior to perimeter control alone and 2) VSL and perimeter control could complement each other to further improve network operations.

Future work will consider multiple exit ramps off the freeway into the urban regions. As discussed in the introduction of this paper, adding exit ramps increases the complexity of the MINLP presented, due to the addition of route choice. Users will have multiple options to exit the freeway, and a route choice model must be developed to account for that choice. Future work will also include internal signal control mechanisms within each region of the urban network. For example, previous work (*30*) has shown the MFD of an urban network changes drastically when left turns are prohibited, making strategic left turn prohibition another possible congestion management strategy to implement alongside VSL and perimeter metering control. A joint strategy that combines three options could provide even superior benefits to the combined mixed freeway-urban network.

ACKNOWLEDGEMENTS

This research was supported by NSF Grant CMMI-1749200.

AUTHOR CONTRIBUTIONS

The authors confirm contribution to the paper as follows: study conception and design: RY, VG; analysis and interpretation of results: RY, VG; draft manuscript preparation: RY, VG. All authors reviewed the results and approved the final version of the manuscript.

REFERENCES

1. Hegyi, A., B. De Schutter, and H. Hellendoorn. Model Predictive Control for Optimal Coordination of Ramp Metering and Variable Speed Limits. *Transportation Research Part C: Emerging Technologies*, Vol. 13, No. 3, 2005, pp. 185–209. https://doi.org/10.1016/J.TRC.2004.08.001.

2. Bellemans, T., B. De Schutter, and B. De Moor. Model Predictive Control for Ramp Metering of Motorway Traffic: A Case Study. *Control Engineering Practice*, Vol. 14, No. 7, 2006, pp. 757–767. https://doi.org/10.1016/J.CONENGPRAC.2005.03.010.

3. Gayah, V. V., C. D. Santos, M. Abdel-Aty, A. Dhindsa, and J. Dilmore. Evaluating ITS Strategies for Real-Time Freeway Safety Improvement. *IEEE Conference on Intelligent Transportation Systems, Proceedings, ITSC*, 2006.

4. Abdel-Aty, M., R. J. Cunningham, V. V. Gayah, and L. Hsia. Dynamic Variable Speed Limit Strategies for Real-Time Crash Risk Reduction on Freeways. *Transportation Research Record*, No. 2078, 2008. https://doi.org/10.3141/2078-15.

5. Chen, D., and S. Ahn. Variable Speed Limit Control for Severe Non-Recurrent Freeway Bottlenecks. *Transportation Research Part C: Emerging Technologies*, Vol. 51, 2015, pp. 210–230. https://doi.org/10.1016/J.TRC.2014.10.015.

6. Han, Y., D. Chen, and S. Ahn. Variable Speed Limit Control at Fixed Freeway Bottlenecks Using Connected Vehicles. *Transportation Research Part B: Methodological*, Vol. 98, 2017, pp. 113–134. https://doi.org/10.1016/J.TRB.2016.12.013.

7. Papageorgiou, M., C. Diakaki, V. Dinopoulou, A. Kotsialos, and Y. Wang. Review of Road Traffic Control Strategies. No. 91, 2003, pp. 2043–2065.

8. Robertson, D. I., and R. D. Bretherton. Optimizing Networks of Traffic Signals in Real Time—The SCOOT Method. *IEEE Transactions on Vehicular Technology*, Vol. 40, No. 1, 1991, pp. 11–15. https://doi.org/10.1109/25.69966.

9. Xie, X. F., S. F. Smith, L. Lu, and G. J. Barlow. Schedule-Driven Intersection Control. *Transportation Research Part C: Emerging Technologies*, Vol. 24, 2012, pp. 168–189. https://doi.org/10.1016/j.trc.2012.03.004.

10. Mirchandani, P., and L. Head. A Real-Time Traffic Signal Control System: Architecture, Algorithms, and Analysis. *Transportation Research Part C: Emerging Technologies*, 2001. https://doi.org/10.1016/S0968-090X(00)00047-4.

11. Godfrey, J. W. The Mechanism of a Road Network. *Traffic Engineering & Control*, Vol. 11, No. 7, 1969, pp. 323–327.

12. Mahmassani, H., J. C. Williams, and R. Herman. Investigation of Network-Level Traffic Flow Relationships: Some Simulation Results. *Transportation Research Record: Journal of the Transportation Research Board*, Vol. 971, 1984, pp. 121–130.

13. Geroliminis, N., and C. F. Daganzo. Existence of Urban-Scale Macroscopic Fundamental Diagrams: Some Experimental Findings. *Transportation Research Part B: Methodological*, Vol. 42, No. 9, 2008, pp. 759–770.

14. Geroliminis, N., and J. Sun. Properties of a Well-Defined Macroscopic Fundamental Diagram for Urban Systems. *Transportation Research Part B*, Vol. 45, No. 3, 2011, pp. 605–617. https://doi.org/10.1016/j.trb.2010.11.004.

15. Daganzo, C. F., V. V. Gayah, and E. J. Gonzales. Macroscopic Relations of Urban Traffic Variables: Bifurcations, Multivaluedness and Instability. *Transportation Research Part B: Methodological*, Vol. 45, No. 1, 2011, pp. 278–288.

16. Daganzo, C. F. Urban Gridlock: Macroscopic Modeling and Mitigation Approaches. *Transportation Research Part B: Methodological*, Vol. 41, No. 1, 2007, pp. 49–62.

17. Haddad, J., and N. Geroliminis. On the Stability of Traffic Perimeter Control in Two-

Region Urban Cities. *Transportation Research Part B: Methodological*, Vol. 46, No. 9, 2012, pp. 1159–1176.

18. Keyvan-Ekbatani, M., A. Kouvelas, I. Papamichail, and M. Papageorgiou. Exploiting the Fundamental Diagram of Urban Networks for Feedback-Based Gating. *Transportation Research Part B: Methodological*, Vol. 46, No. 10, 2012, pp. 1393–1403.

19. Aboudolas, K., and N. Geroliminis. Perimeter and Boundary Flow Control in Multi-Reservoir Heterogeneous Networks. *Transportation Research Part B: Methodological*, Vol. 55, 2013, pp. 265–281.

20. Haddad, J., and Z. Zheng. Adaptive Perimeter Control for Multi-Region Accumulation-Based Models with State Delays. *Transportation Research Part B: Methodological*, 2018. https://doi.org/10.1016/j.trb.2018.05.019.

21. Yang, K., M. Menendez, and N. Zheng. Heterogeneity Aware Urban Traffic Control in a Connected Vehicle Environment: A Joint Framework for Congestion Pricing and Perimeter Control. *Transportation Research Part C: Emerging Technologies*, Vol. 105, 2019, pp. 439–455. https://doi.org/10.1016/j.trc.2019.06.007.

22. Haitao, H., K. Yang, H. Liang, M. Menendez, and S. I. Guler. Providing Public Transport Priority in the Perimeter of Urban Networks: A Bimodal Strategy. *Transportation Research Part C: Emerging Technologies*, Vol. 107, 2019, pp. 171–192. https://doi.org/10.1016/j.trc.2019.08.004.

23. Geroliminis, N., and D. M. Levinson. Cordon Pricing Consistent with the Physics of Overcrowding. In *18th International Symposium on Transportation and Traffic Theory*, Springer.

24. Gonzales, E. J., and C. F. Daganzo. Morning Commute with Competing Modes and Distributed Demand: User Equilibrium, System Optimum, and Pricing. *Transportation Research Part B: Methodological*, Vol. 46, No. 10, 2012, pp. 1519–1534.

25. Simoni, M. D., A. J. Pel, R. A. Waraich, and S. P. Hoogendoorn. Marginal Cost Congestion Pricing Based on the Network Fundamental Diagram. *Transportation Research Part C: Emerging Technologies*, Vol. 56, 2015, pp. 221–238.

26. Zheng, N., R. A. Waraich, K. W. Axhausen, and N. Geroliminis. A Dynamic Cordon Pricing Scheme Combining the Macroscopic Fundamental Diagram and an Agent-Based Traffic Model. *Transportation Research Part A: Policy and Practice*, Vol. 46, No. 8, 2012, pp. 1291–1303.

27. Gayah, V. V., and C. F. Daganzo. Analytical Capacity Comparison of One-Way and Two-Way Signalized Street Networks. *Transportation Research Record: Journal of the Transportation Research Board*, No. 2301, 2012, pp. 76–85.

28. Ortigosa, J., V. V. Gayah, and M. Menendez. Analysis of One-Way and Two-Way Street Configurations on Urban Grids. *Transportmetrica B: Transport Dynamics*, Vol. 7, No. 1, 2019, pp. 61–81.

29. Ortigosa, J., V. V. Gayah, and M. Menendez. Analysis of Network Exit Functions for Various Urban Grid Network Configurations. *Transportation Research Record: Journal of the Transportation Research Board*, No. 2491, 2015, pp. 12–21.

30. DePrator, A., O. Hitchcock, and V. V. Gayah. Improving Urban Street Network Efficiency by Prohibiting Left Turns at Signalized Intersections. *Transportation Research Record: Journal of the Transportation Research Board*, Vol. 2622, No. 1, 2017, pp. 58–69.

31. Knoop, V. L., S. P. Hoogendoorn, and J. W. C. Van Lint. Routing Strategies Based on Macroscopic Fundamental Diagram. *Transportation Research Record: Journal of the Transportation Research Board*, Vol. 2315, No. 1, 2012, pp. 1–10.

32. Yildirimoglu, M., and N. Geroliminis. Approximating Dynamic Equilibrium Conditions with Macroscopic Fundamental Diagrams. *Transportation Research Part B: Methodological*, Vol. 70, 2014, pp. 186–200.

33. Haddad, J., M. Ramezani, and N. Geroliminis. Cooperative Traffic Control of a Mixed Network with Two Urban Regions and a Freeway. *Transportation Research Part B: Methodological*, Vol. 54, 2013, pp. 17–36.

34. Ji, Y., and N. Geroliminis. On the Spatial Partitioning of Urban Transportation Networks. *Transportation Research Part B: Methodological*, Vol. 46, No. 10, 2012, pp. 1639–1656.

35. Cho, H., and Y. Kim. Analysis of Traffic Flow with Variable Speed Limit on Highways. *KSCE Journal of Civil Engineering*, Vol. 16, No. 6, 2012, pp. 1048–1056. https://doi.org/10.1007/s12205-012-1395-x.

36. Lighthill, M. J., and G. B. Whitham. On Kinematic Waves. I. Flood Movement in Long Rivers. *Proceedings of the Royal Society of London. Series A. Mathematical and Physical Sciences*, Vol. 229, No. 1178, 1955, pp. 281–316.

37. Lighthill, M. J., and G. B. Whitham. On Kinematic Waves. II. A Theory of Traffic Flow on Long Crowded Roads. *Proceedings of the Royal Society of London. Series A. Mathematical and Physical Sciences*, Vol. 229, No. 1178, 1955, pp. 317–345.

38. Richards, P. I. Shock Waves on the Highway. *Operations Research*, Vol. 4, No. 1, 1956, pp. 42–51.

39. Gayah, V. V., E. T. Donnell, Z. Yu, and L. Li. Safety and Operational Impacts of Setting Speed Limits below Engineering Recommendations. *Accident Analysis and Prevention*, Vol. 121, 2018, pp. 43–52. https://doi.org/10.1016/j.aap.2018.08.029.

40. Geroliminis, N., J. Haddad, M. Ramezani, and N. Geroliminis. Optimal Perimeter Control for Two Urban Regions with Macroscopic Fundamental Diagrams: A Model Predictive Approach. *Intelligent Transportation Systems, IEEE Transactions on*, Vol. 14, No. 1, 2013, pp. 348–359.

41. Kennedy, J., and R. Eberhart. Particle Swarm Optimization. No. 4, pp. 1942–1948.

42. Shokrian, M., and K. A. High. Application of a Multi Objective Multi-Leader Particle Swarm Optimization Algorithm on NLP and MINLP Problems. *Computers and Chemical Engineering*, Vol. 60, 2014, pp. 57–75. https://doi.org/10.1016/j.compchemeng.2013.08.004.